

A General Approach for Producing Hamiltonian Numerical Schemes for Fluid Equations

Colin Cotter

February 8, 2020

Abstract

Given a fluid equation with reduced Lagrangian l which is a functional of velocity u and advected density D given in Eulerian coordinates, we give a general method for semidiscretising the equations to give a canonical Hamiltonian system; this system may then be integrated in time using a symplectic integrator. The method is Lagrangian, with the variables being a set of Lagrangian particle positions and their associated momenta. The canonical equations obtained yield a discrete form of Euler-Poincaré equations for l when projected onto the grid, with a new form of discrete calculus to represent the gradient and divergence operators. Practical symplectic time integrators are suggested for a large family of equations which include the shallow-water equations, the EP-Diff equations and the 3D compressible Euler equations, and we illustrate the technique by showing results from a numerical experiment for the EP-Diff equations.

Contents

1	Introduction	1
2	Background	3
3	Canonical Hamiltonian particle-mesh semidiscretisations	5
4	Symplectic time integration methods	9
5	Examples	10
5.1	Example: the shallow-water- α equations	10
5.2	Example: the 2D EP-Diff equations	12
6	Numerical results	13
7	Discussion and outlook	14

1 Introduction

There has been much recent interest in obtaining Hamiltonian methods for the various equations of motion for fluids (such as the shallow-water equations, and the 2D Euler equations). The Hamiltonian method programme consists of two stages:

1. Take a Hamiltonian PDE with Hamiltonian \mathcal{H} and structure operator \mathcal{J} so that the equation takes the form

$$\mathcal{J}z_t(x) = \frac{\delta \mathcal{H}}{\delta z}.$$

Discretise the Hamiltonian and the structure operator to obtain a finite dimensional Hamiltonian \hat{H} and symplectic structure matrix \hat{J} to give a finite dimensional Hamiltonian system

$$\hat{J}\dot{z} = \frac{\partial \hat{H}}{\partial z}.$$

2. Discretise the finite dimensional system in time using a symplectic integrator (for a general review of symplectic methods see (HLW02) or (LR05)).

The advantage of this approach is that the symplectic integrator will guarantee excellent long-time conservation properties (BG94; Hai94; HL97; Rei99) with the spatially-discrete Hamiltonian \hat{H} satisfying

$$|\hat{H}(t) - \hat{H}(0)| < c_1 \delta t^p, \quad |t| < c_2 e^{-c_3/\delta t},$$

where p is the order of the symplectic method in time and where c_1 , c_2 and c_3 are positive constants. Note that Hamiltonian methods are not the same as multi-symplectic integrators (MPS98; MPSW01; Rei00; MR03b; MR03a) where the Lagrangian is symmetrically discretised in time and space, and discrete variations are taken to obtain the numerical method, which then offers additional symmetry properties (OWW04).

In general it has been very difficult to obtain discrete structure operators \hat{J} which satisfy the Jacobi identity and progress has only been made for Hamiltonian PDEs with canonical structure (with a few exceptions *e.g.* (Zei91)). In the context of fluid equations this means that the equations must be solved in Lagrangian coordinates where the symplectic structure is canonical. For the case of 2D incompressible flow this leads to methods where Lagrangian particles carry vorticity instead of mass, either as Dirac δ -functions (point-vortex methods (CK00, for a review)) or in “blobs” surrounding the particle (vortex-blob methods (Cho73; OS01; CR04b)). For the case of compressible flow the particles carry masses which are interpolated through basis functions to the entire domain to give the density field; this type of discretisation is called Smoothed-Particle Hydrodynamics (SPH) (GM77; Luc77; Sal83). The related Hamiltonian Particle-Mesh (HPM) method (FGR02; CFR03; FR04; CR04a) discretises a regularised form of the equations (with the regularisation operator discretised on an Eulerian grid) so that good long-time behaviour is obtained when the finite dimensional system is integrated with a symplectic integrator (this is described further in section 2).

The difficulty with Lagrangian coordinates is that the equations can become very complicated (especially when differential operators in Eulerian coordinates are involved). Analytically, the most tractable approach is to transform the Lagrangian L for the flow maps in Lagrangian coordinates to a reduced Lagrangian l for the velocity field $u(x)$ in Eulerian coordinates, and then to use the Euler-Poincaré (EP) equations (HMR98a; HMR98b) for u which are equivalent to the canonical Hamilton's equations for the Lagrangian variables. Writing the reduced Lagrangian which integrates over Eulerian coordinates means that the equations are much easier to handle. This greatly aids model derivation (Hol02), analysis (MRS00; MS01; Shk02), model reduction (HZ98; Oli05) and averaging (Hol99); it is clear that it would be attractive to use the reduced Lagrangian to derive numerical methods too. However, in the case of general fluid equations this would mean losing the canonical structure operator because the Legendre transform in Eulerian coordinates results in a non-canonical Lie-Poisson equation.

In this paper we give a general approach, using Lagrangian variables so that there is a canonical structure operator which is easy to discretise, whilst evaluating the Hamiltonian on an Eulerian grid. This approach fully develops a dual grid-particle approach (as an extension of the mixed form that HPM uses with the potential energy in Eulerian variables whilst the kinetic energy is in Lagrangian variables). The particle-mesh formulation allows quantities (such as momentum and density) which are given at the particle locations, to be interpolated to the Eulerian grid. The Hamiltonian is then approximated as a sum over the Eulerian grid points, and Theorem 3.3 in this paper shows that the canonical equations obtained from the discrete Hamiltonian produce a set of discrete EP equations on the grid (although computationally the equations are treated in Lagrangian form). It then remains to apply a numerical time-stepping algorithm which preserves the canonical symplectic structure.

The structure of the rest of the paper is as follows: section 2 provides some background on SPH and HPM to prepare the way for the general approach to obtaining semidiscretisations. This approach is set out, together with the statement and proof of Theorem 3.3, in section 3, and suitable symplectic time-integrators are suggested in section 4. The next two sections show how to apply the approach in two examples: the shallow-water- α equations in section 5.1, and the 2D EP-Diff equation in section 5.2. Both of these examples are in 2-dimensional geometry although the approach is completely general and may be used to discretise n -dimensional PDEs. Section 6 gives some numerical results for the 2D EP-Diff equation and section 7 contains some brief final discussion.

2 Background

HPM was originally introduced in (FGR02) as a semidiscretisation of the regularised layer-depth shallow-water (RLDSW) equations:

$$\mathbf{u}_t + \mathbf{u} \cdot \nabla \mathbf{u} = -g \nabla (1 - \alpha^2 \Delta)^{-1} D, \quad D_t + \nabla \cdot (D \mathbf{u}) = 0.$$

The success of this method is based on its “dual picture” nature, as the Lagrangian particle dynamics provides a canonical symplectic structure (which is easy to treat numerically using symplectic integrators) whilst the inverse modified Helmholtz operator takes its simplest form on the Eulerian grid.

HPM can be viewed as a modification of SPH (GM77; Luc77) which is a Lagrangian particle method for compressible flow. In the SPH method for shallow-water, the layer-depth D is represented by a linear combination of radial basis functions which are centred on a finite set $\{\mathbf{X}_\beta(t)\}_{\beta=1}^n$ of Lagrangian particles:

$$D(\mathbf{x}, t) = \frac{1}{\Delta S} \sum_{\beta=1}^n D_\beta \phi(\mathbf{x} - \mathbf{X}_\beta(t)),$$

where ϕ is a radial basis function with integral ΔS , and $\{D_\beta\}_{\beta=1}^n$ are constant weights. Other fields $f(\mathbf{x}, t)$ (such as temperature, velocity *etc.*) may be interpolated from the values $\{f_\beta(t)\}_{\beta=1}^n$ at the particle locations to the entire domain *via* the product

$$D(\mathbf{x}, t) f(\mathbf{x}, t) = \frac{1}{\Delta S} \sum_{\beta=1}^n D_\beta f_\beta(t) \phi(\mathbf{x} - \mathbf{X}_\beta(t)).$$

This interpolation may then be used to establish the continuity equation for h :

$$\begin{aligned} \partial_t D(\mathbf{x}, t) &= \frac{1}{\Delta S} \partial_t \sum_{\beta=1}^n D_\beta \phi(\mathbf{x} - \mathbf{X}_\beta(t)), \\ &= \frac{1}{\Delta S} \sum_{\beta=1}^n D_\beta \dot{\mathbf{X}}_\beta(t) \nabla_{\mathbf{X}_\beta} \phi(\mathbf{x} - \mathbf{X}_\beta(t)), \\ &= -\frac{1}{\Delta S} \sum_{\beta=1}^n D_\beta \dot{\mathbf{X}}_\beta(t) \nabla_{\mathbf{x}} \phi(\mathbf{x} - \mathbf{X}_\beta(t)), \\ &= -\nabla_{\mathbf{x}} \cdot \frac{1}{\Delta S} \sum_{\beta=1}^n D_\beta \dot{\mathbf{X}}_\beta(t) \phi(\mathbf{x} - \mathbf{X}_\beta(t)), \\ &= -\nabla_{\mathbf{x}} \cdot (D \mathbf{v}(\mathbf{x}, t)), \end{aligned}$$

where $\nabla_{\mathbf{X}_\beta}$ is the gradient with respect to \mathbf{X}_β , $\nabla_{\mathbf{x}}$ is the gradient with respect to \mathbf{x} , and $\mathbf{v}(\mathbf{x}, t)$ is the interpolation of the particle velocities $\dot{\mathbf{X}}_\beta$ to the entire domain.

In SPH methods, the forces on the particles are simply evaluated by interpolating the forces to the entire domain and then substituting the particle positions in the formula. These methods are thus mesh-free which makes them popular with astrophysicists who are able to model self-gravitating fluids (such as colliding stars and accretion discs) contained in an infinite vacuum simply by giving the basis functions finite support so that there is no density in the far-field. In particle-mesh methods, however, the aim is to meet the need for easy evaluation of Eulerian differential operators such as the inverse modified Helmholtz operator in the RLDSW equations. For a general mesh with m grid points $\{\mathbf{x}_k\}_{k=1}^m$, the layer-depth D_k at grid point k is given by

$$D(\mathbf{x}_k, t) = \frac{1}{\Delta S} \sum_{\beta=1}^n D_\beta \psi_k(\mathbf{X}_\beta),$$

where

$$\psi_k(\mathbf{X}) = \phi(\mathbf{x}_k; \mathbf{X}),$$

and $\phi(\mathbf{x}; \mathbf{X}_\beta)$ is some general basis function (such as a radial basis function or a Cartesian product of 1D basis functions) centred on \mathbf{X}_β that satisfies

$$\nabla_{\mathbf{x}} \phi(\mathbf{x}; \mathbf{X}) = -\nabla_{\mathbf{X}} \phi(\mathbf{x}; \mathbf{X}), \quad \int \phi(\mathbf{x}; \mathbf{0}) d^2 x = \Delta S.$$

The key to the method is the restriction to basis functions (such as the Cartesian product of cubic B-splines (dB78, for example)) which satisfy the partition of unity property:

$$\sum_{\beta=1}^n \psi_k(\mathbf{x}) = 1 \quad \forall \mathbf{x}$$

which means that any quantity f may be interpolated from the grid to the whole domain:

$$f(\mathbf{x}) = \sum_{k=1}^m f(\mathbf{x}_k) \psi_k(\mathbf{x}).$$

This allows us to interpolate from the grid to the particles *via*

$$f_\beta = f(\mathbf{X}_\beta) = \sum_{k=1}^m f(\mathbf{x}_k) \psi_k(\mathbf{X}_\beta).$$

The gradient of the density can be obtained by taking the gradient of the basis functions evaluated at the particle positions:

$$\begin{aligned} \nabla_{\mathbf{x}} D(\mathbf{x})|_{\mathbf{x}=\mathbf{X}_\beta} &= - \sum_{k=1}^m D(\mathbf{x}_k) \nabla_{\mathbf{X}_\beta} \psi_k(\mathbf{X}_\beta) \\ &= - \sum_{k=1}^m \nabla_{\mathbf{X}_\beta} \psi_k(\mathbf{X}_\beta) \frac{1}{\Delta S} \sum_{\gamma=1}^n D_\gamma \psi_k(\mathbf{X}_\gamma). \end{aligned}$$

The RLDSW equations were originally introduced after failed attempts to exploit the canonical Hamiltonian structure of SPH (applied to the SW equations) by performing the time integration using a symplectic method (with the aim of obtaining long time approximate preservation of energy, momentum and adiabatic invariants). These attempts failed because computational efficiency necessitates the use of basis functions with compact support. When the flow is nearly incompressible (e.g. when the system is near to geostrophic balance in the rotating case) the basis functions supported local compressible oscillations which quickly destabilised the flow and led to equipartition of energy much too quickly. The smoothing operator applied to the layer depth means that the local basis functions become global and the small oscillations are filtered out in the momentum equation. The semi-discretised equations are:

$$\begin{aligned} \dot{\mathbf{V}}_\beta &= g \sum_{k=1}^m \nabla_{\mathbf{X}_\beta} \psi_k(\mathbf{X}_\beta) \sum_{l=1}^m (A^{-1})_{kl} \frac{1}{\Delta S} \sum_{\gamma=1}^n \psi_k(\mathbf{X}_\gamma) D_\gamma, \\ \dot{\mathbf{X}}_\beta &= \mathbf{V}_\beta, \quad \beta = 1, \dots, n, \end{aligned}$$

where A is the numerical approximation to the modified Helmholtz operator (obtained using e.g. Fourier series or finite elements). These equations have a canonical Hamiltonian structure with Hamiltonian

$$H = \sum_{\beta=1}^n \frac{|\mathbf{m}_\beta|^2}{2D_\beta} + g \sum_{k,l=1}^m \frac{1}{\Delta S} \sum_{\beta,\gamma=1}^n \psi_k(\mathbf{X}_\beta) (A^{-1})_{kl} D_\gamma \psi_l(\mathbf{X}_\gamma),$$

where the momentum is given by

$$\mathbf{m}_\beta = D_\beta \mathbf{v}_\beta, \quad \beta = 1, \dots, n.$$

These equations may be integrated using the symplectic Störmer-Verlet method because the Hamiltonian splits into separate functions of $\{\mathbf{m}\}_{\beta=1}^n$ and $\{\mathbf{X}\}_{\beta=1}^n$ (as in classical mechanics) (McL99).

In this method, the potential energy is obtained by interpolating the height field to the grid and summing over the gridpoints, whilst the kinetic energy is evaluated in Lagrangian coordinates only. In the next section we shall extend the approach to the kinetic energy used here by evaluating the entire Hamiltonian on the Eulerian grid.

3 Canonical Hamiltonian particle-mesh semidiscretisations

Throughout this section, and for the rest of this paper, we shall adopt the notation that a bar indicates a quantity stored at a particle location e.g. \overline{m} , \overline{D} , etc., and a tilde indicates a quantity stored at a grid location e.g. \tilde{m} , \tilde{D} , \tilde{u} . Also, Greek letters will be used for indices denoting the particle numbering, e.g. momentum \overline{m}_β at particle \mathbf{X}_β , whilst Roman letters will be used for indices denoting the grid numbering, e.g. velocity \tilde{u}_k at grid point \mathbf{x}_k .

The programme for producing Hamiltonian particle-mesh semidiscretisations is as follows:

1. Start with the reduced Lagrangian l for the EP equations given in Eulerian coordinates. This method applies to semi-direct product systems where the l is a functional of the velocity \mathbf{u} and the density D (which satisfies the continuity equation). In this section we shall look at PDEs in two dimensions, but the extension to higher (and lower) dimensions is straightforward.
2. To obtain the discrete Lagrangian \hat{L} , take the continuous Lagrangian l which is written as an integral over \mathcal{D}

$$l = \int \lambda(\mathbf{u}, D) d^2x,$$

where λ is a nonlinear operator, and replace it with a sum over gridpoints

$$\hat{L} = \sum_{kl} M_{kl} \lambda_k \left(\{\tilde{u}_l\}_{l=1}^m, \{\tilde{D}_l\}_{l=1}^m \right),$$

where M is the matrix representing the approximation to integration (often referred to in the finite-element literature as the mass matrix) and where λ_k is a function approximating λ at the point \mathbf{x}_k , with any differential operators being replaced by matrix operations on the grid in the manner consistent with the choice of M .

3. Use the Legendre transform

$$\hat{H}(\{\tilde{m}_l\}_{l=1}^m, \{\tilde{D}_l\}_{l=1}^m) = \sum_{kl} M_{kl} \tilde{u}_k \cdot \tilde{m}_k - \hat{L},$$

where

$$\sum_l M_{kl} \tilde{m}_l = \frac{\partial \hat{L}}{\partial \tilde{u}_k}, \quad (1)$$

to obtain the Hamiltonian written in Eulerian coordinates.

4. Take n Lagrangian particles $\{\mathbf{X}_\beta\}_{\beta=1}^n$ together with m Eulerian grid points $\{\mathbf{x}_k\}_{k=1}^m$ on the domain \mathcal{D} and a set of basis functions $\psi_k(\mathbf{x})$ defined by

$$\psi_k(\mathbf{x}) = \phi(\mathbf{x}_k; \mathbf{x}),$$

with the partition-of-unity property

$$\sum_k \psi_k(\mathbf{x}) = 1 \text{ for all } \mathbf{x} \in \mathcal{D}.$$

and where ϕ satisfies

$$\nabla_{\mathbf{x}} \phi(\mathbf{y}; \mathbf{x}) = -\nabla_{\mathbf{y}} \phi(\mathbf{y}; \mathbf{x}), \quad \int_{\mathcal{D}} \phi(\mathbf{x}; \mathbf{y}) d^2x = \Delta S,$$

This property allows grid values $f(\mathbf{x}_k)$ to be interpolated to the whole domain \mathcal{D} :

$$f(\mathbf{x}) = \sum_k f(\mathbf{x}_k) \psi_k(\mathbf{x}),$$

as well as gradients:

$$\nabla f(\mathbf{x}) = \sum_k f(\mathbf{x}_k) \nabla \psi_k(\mathbf{x}).$$

Here we avoid the issue of boundary conditions by stipulating that \mathcal{D} is a closed, compact manifold (e.g. a square with periodic boundaries).

5. Give the β -th particle a momentum density $\bar{\mathbf{m}}_\beta$ and a constant layer-depth density \bar{D}_β (which will be identified as a conserved mass in the particle system that is obtained after semidiscretisation). Interpolate the layer-depth density and momentum density to the grid using

$$\sum_l M_{kl} \tilde{\mathbf{m}}_l = \sum_\beta \frac{\bar{\mathbf{m}}_\beta}{\Delta S} \psi_k(\mathbf{X}_\beta), \quad \sum_{kl} M_{kl} \tilde{D}_l = \sum_\beta \frac{\bar{D}_\beta}{\Delta S} \psi_k(\mathbf{X}_\beta). \quad (2)$$

The mass matrix is present because the product of the momentum $\bar{\mathbf{m}}$ with the basis functions ψ should be interpreted as the approximation to the one-form density $\mathbf{m} d^2 x$; inverting the mass matrix “strips off” the density $d^2 x$.

6. The equations of motion for the particle positions $\{\mathbf{X}_\beta\}_{\beta=1}^n$ and their associated local momenta $\{\bar{\mathbf{m}}_\beta/\Delta S\}_{\beta=1}^n$ are then the canonical Hamilton's equations for this discrete Hamiltonian (1) having applied the substitution in equations (2).

Now we shall show that the equations of motion represent an approximation to the EP equations. First, we make a few definitions which set out our discrete calculus which is used to form the discrete EP equations.

Definition 3.1. For a quantity \tilde{f} specified on the grid, define the grid-to-particle map by interpolating to the whole of \mathcal{D} ,

$$f(\mathbf{x}) = \sum_k \tilde{f}_k \psi_k(\mathbf{x}),$$

and evaluating at the particle positions

$$f(\mathbf{X}_i) = \sum_k \tilde{f}_k \psi_k(\mathbf{X}_i).$$

We shall use the following notation

$$[\tilde{f}]_\beta = \sum_k \tilde{f}_k \psi_k(\mathbf{X}_\beta).$$

Further define the grid-to-particle gradient map applied to \tilde{f} by interpolating to the whole of \mathcal{D} ,

$$f(\mathbf{x}) = \sum_k \tilde{f}_k \psi_k(\mathbf{x}),$$

taking a gradient,

$$\nabla f(\mathbf{x}) = \sum_k \tilde{f}_k \nabla \psi_k(\mathbf{x}),$$

and evaluating at the particle positions

$$\nabla f(\mathbf{X}_\beta) = \sum_k \tilde{f}_k \nabla \psi_k(\mathbf{X}_\beta).$$

We shall use the following notation

$$[\nabla \tilde{f}]_\beta = \sum_k \tilde{f}_k \nabla \psi_k(\mathbf{X}_\beta).$$

Definition 3.2. For a density \bar{f} specified on the particle locations, define the particle-to-grid map that interpolates to the grid by

$$\sum_{kl} M_{kl} \langle \bar{f} \rangle_l = \sum_\beta \frac{\bar{f}_\beta}{\Delta S} \psi_k(\mathbf{X}_\beta).$$

Also for a function \tilde{g} specified on the grid, use the following notation for the interpolated product:

$$\sum_{kl} M_{kl} \langle \bar{f}[\tilde{g}] \rangle_l = \sum_\beta \frac{\bar{f}_\beta}{\Delta S} [\tilde{g}]_\beta \psi_k(\mathbf{X}_\beta).$$

For a one-form density $\bar{\mathbf{f}}$ specified on the particle locations, further define the particle-to-grid divergence map on the grid by

$$\sum_l M_{kl} \langle \nabla \cdot \bar{\mathbf{f}} \rangle_l = - \sum_\beta \frac{\bar{\mathbf{f}}_\beta}{\Delta S} \nabla \psi_k(\mathbf{X}_\beta).$$

This map is the adjoint to the grid-to-particle gradient map.

These interpolation maps represent the whole key to the approach: they allow the dynamical equations to be interpreted either on the grid or on the particle positions. In particular, the canonical symplectic structure is used to derive the particle dynamics (and so most of the focus computationally will be on the particle variables) whilst the Eulerian interpretation makes it possible to solve for the velocity given the momentum on the grid. The following theorem shows that the equations on the grid can be interpreted as a discrete EP equation:

Theorem 3.3. *On the grid the equations of motion obtained from this procedure take the following form*

$$\frac{d}{dt} \langle \bar{\mathbf{m}} \rangle_k + \langle \nabla \cdot ([\tilde{\mathbf{u}}] \bar{\mathbf{m}}) \rangle_k + \langle [(\nabla \tilde{\mathbf{u}})^T] \cdot \bar{\mathbf{m}} \rangle_k = \left\langle \bar{D} \left[M^{-1} \nabla \frac{\partial \hat{L}}{\partial \bar{D}} \right] \right\rangle_k, \quad (3)$$

$$\partial_t \langle \bar{D} \rangle_k + \langle \nabla \cdot (\bar{D} [\tilde{\mathbf{u}}]) \rangle_k = 0, \quad (4)$$

$$\langle \bar{\mathbf{m}} \rangle_k = \sum_l (M^{-1})_{kl} \frac{\partial \hat{L}}{\partial \tilde{\mathbf{u}}_l}, \quad (5)$$

which gives an approximation on the grid, using the discrete calculus defined above, to the EP equations:

$$\begin{aligned} \partial_t \mathbf{m} + \nabla \cdot (\mathbf{u} \mathbf{m}) + (\nabla \mathbf{u})^T \cdot \mathbf{m} &= D \nabla \frac{\delta l}{\delta D}, \\ \partial_t D + \nabla \cdot (\mathbf{u} D) &= 0, \\ \mathbf{m} &= \frac{\delta l}{\delta \mathbf{u}}. \end{aligned}$$

Furthermore, at the particle locations the equations takes the form

$$\frac{d}{dt} \frac{\bar{\mathbf{m}}_\beta}{\bar{D}_\beta} + [(\nabla \tilde{\mathbf{u}})^T]_\beta \cdot \frac{\bar{\mathbf{m}}_\beta}{\bar{D}_\beta} = \left[M^{-1} \nabla \frac{\partial \hat{L}}{\partial \bar{D}} \right]_\beta, \quad (6)$$

$$\frac{d}{dt} \mathbf{X}_\beta = [\tilde{\mathbf{u}}]_\beta, \quad (7)$$

which gives an approximation at the particle locations to the EP equation in vector form:

$$\begin{aligned} \frac{D}{Dt} \frac{\mathbf{m}}{D} + (\nabla \mathbf{u})^T \cdot \frac{\mathbf{m}}{D} &= \nabla \frac{\delta L}{\delta D}, \\ \frac{D}{Dt} &= (\partial_t + \mathbf{u} \cdot \nabla). \end{aligned}$$

Proof. The \mathbf{X} equation obtained is

$$\begin{aligned} \dot{\mathbf{X}}_\beta &= \Delta S \nabla \bar{\mathbf{m}}_\beta \hat{H}, \\ &= \sum_k \left((\nabla \bar{\mathbf{m}}_\beta \sum_l M_{kl} \tilde{\mathbf{m}}_l) \cdot \tilde{\mathbf{u}}_k + (\nabla \bar{\mathbf{m}}_\beta \tilde{\mathbf{u}}_k) \cdot \sum_l M_{kl} \tilde{\mathbf{m}}_l \right) - \nabla \bar{\mathbf{m}}_\beta \hat{L}. \end{aligned}$$

These three terms may be expanded out:

$$\sum_k \left(\nabla \bar{\mathbf{m}}_\beta \sum_l M_{kl} \tilde{\mathbf{m}}_l \right) \cdot \tilde{\mathbf{u}}_k = \sum_k \left(\nabla \bar{\mathbf{m}}_\beta \sum_\gamma \bar{\mathbf{m}}_\gamma \psi_k(\mathbf{X}_\gamma) \right) \cdot \tilde{\mathbf{u}}_k$$

$$\begin{aligned}
&= \sum_k \tilde{\mathbf{u}}_k \psi_k(\mathbf{X}_\beta), \\
\sum_k (\nabla_{\bar{\mathbf{m}}_\beta} \tilde{\mathbf{u}}_k) \cdot \sum_l M_{kl} \tilde{\mathbf{m}}_l &= \sum_{klm} (\nabla_{\tilde{\mathbf{m}}_l} \tilde{\mathbf{u}}_k) \cdot M_{km} \tilde{\mathbf{m}}_m \psi_l(\mathbf{X}_\beta), \\
\nabla_{\bar{\mathbf{m}}_\beta} \hat{L} &= \sum_{kl} (\nabla_{\tilde{\mathbf{m}}_l} \tilde{\mathbf{u}}_k) \cdot (\nabla_{\tilde{\mathbf{u}}_k} \hat{L}) \psi_l(\mathbf{X}_\beta), \\
&= \sum_{klm} (\nabla_{\tilde{\mathbf{m}}_l} \tilde{\mathbf{u}}_k) \cdot M_{kl} \tilde{\mathbf{m}}_m \psi_l(\mathbf{X}_\beta),
\end{aligned}$$

where we have made use of

$$\nabla_{\tilde{\mathbf{u}}_k} \hat{L} = \sum_l M_{kl} \tilde{\mathbf{m}}_l.$$

This means that the second and third terms cancel and the \mathbf{X} equation becomes

$$\dot{\mathbf{X}}_\beta = \sum_k \tilde{\mathbf{u}}_k \psi_k(\mathbf{X}_\beta) = [\tilde{\mathbf{u}}]_\beta.$$

The $\bar{\mathbf{m}}$ equation is

$$\begin{aligned}
\frac{\dot{\bar{\mathbf{m}}}_\beta}{\Delta S} &= -\nabla_{\mathbf{X}_\beta} \hat{H}, \\
&= \sum_{kl} ((\nabla_{\mathbf{X}_\beta} M_{kl} \tilde{\mathbf{m}}_l) \cdot \tilde{\mathbf{u}}_k + (\nabla_{\mathbf{X}_\beta} \tilde{\mathbf{u}}_k) \cdot M_{kl} \tilde{\mathbf{m}}_l) - \nabla_{\mathbf{X}_\beta} \hat{L}.
\end{aligned}$$

Once again, expand these three terms

$$\begin{aligned}
\sum_{kl} (\nabla_{\mathbf{X}_\beta} M_{kl} \tilde{\mathbf{m}}_l) \cdot \tilde{\mathbf{u}}_k &= \sum_k \tilde{\mathbf{u}}_k \cdot \frac{\bar{\mathbf{m}}_\beta}{\Delta S} \nabla_{\mathbf{X}_\beta} \psi_k(\mathbf{X}_\beta), \\
\sum_{kl} (\nabla_{\mathbf{X}_\beta} \tilde{\mathbf{u}}_k) \cdot M_{kl} \tilde{\mathbf{m}}_l &= \sum_{klm} \left(\frac{\bar{\mathbf{m}}_\beta}{\Delta S} \cdot (\nabla_{\tilde{\mathbf{m}}_l} \tilde{\mathbf{u}}_k) \cdot M_{km} \tilde{\mathbf{m}}_m \right) \nabla_{\mathbf{X}_\beta} \psi_l(\mathbf{X}_\beta), \\
\nabla_{\mathbf{X}_\beta} \hat{L} &= \sum_{kl} \left(\frac{\bar{\mathbf{m}}_\beta}{\Delta S} \cdot (\nabla_{\tilde{\mathbf{m}}_l} \tilde{\mathbf{u}}_k) \cdot \nabla_{\tilde{\mathbf{u}}_k} \hat{L} \right) \nabla_{\mathbf{X}_\beta} \psi_l(\mathbf{X}_\beta) \\
&\quad - \sum_k \frac{\partial \hat{L}}{\partial \tilde{D}_k} \nabla_{\mathbf{X}_\beta} \tilde{D}_k, \\
&= \sum_{klm} \left(\frac{\bar{\mathbf{m}}_\beta}{\Delta S} \cdot (\nabla_{\tilde{\mathbf{m}}_l} \tilde{\mathbf{u}}_k) \cdot M_{km} \tilde{\mathbf{m}}_m \right) \nabla_{\mathbf{X}_\beta} \psi_l(\mathbf{X}_\beta) \\
&\quad - \frac{\bar{D}_\beta}{\Delta S} \sum_{kl} \frac{\partial \hat{L}}{\partial \tilde{D}_k} (M^{-1})_{kl} \nabla_{\mathbf{X}_\beta} \psi_l(\mathbf{X}_\beta).
\end{aligned}$$

The \mathbf{m} equation may then be written in the form

$$\frac{d}{dt} \bar{\mathbf{m}}_\beta = -[(\nabla \tilde{\mathbf{u}})^T]_\beta \cdot \bar{\mathbf{m}}_\beta + \bar{D}_\beta \left[\nabla M^{-1} \frac{\partial \hat{L}}{\partial \tilde{D}} \right]_\beta,$$

and dividing through by \bar{D}_β gives equations (6-7).

To obtain equation (3), take the time derivative of $\langle \bar{\mathbf{m}} \rangle_k$:

$$\begin{aligned}
\frac{d}{dt} \sum_l M_{kl} \langle \bar{\mathbf{m}} \rangle_l &= \sum_k \left(\frac{d}{dt} \frac{\bar{\mathbf{m}}_\beta}{\Delta S} \right) \psi_k(\mathbf{X}_\beta) + \frac{1}{(\Delta x)^2} \sum_k \frac{\bar{\mathbf{m}}_\beta}{\Delta S} \frac{d}{dt} \psi_k(\mathbf{X}_\beta), \\
&= \sum_l M_{kl} \left\langle \frac{d}{dt} \bar{\mathbf{m}} \right\rangle_l + \sum_k \frac{\bar{\mathbf{m}}_\beta}{\Delta S} \frac{d}{dt} \mathbf{X}_\beta \cdot \nabla \psi_k(\mathbf{X}_\beta), \\
&= -\sum_l M_{kl} \left(\left\langle [(\nabla \tilde{\mathbf{u}})^T] \cdot \bar{\mathbf{m}} \right\rangle_l + \left\langle \bar{D} \left[\nabla M^{-1} \frac{\partial \hat{L}}{\partial \tilde{D}} \right] \right\rangle_l \right) -
\end{aligned}$$

$$\langle \nabla \cdot (\overline{\mathbf{m}}[\tilde{\mathbf{u}}]) \rangle_l \Big),$$

and dividing by M gives the result. Similarly, equation (4) follows by taking the time derivative of $\langle \overline{D} \rangle_k$:

$$\begin{aligned} \frac{d}{dt} \sum_l M_{kl} \langle \overline{D} \rangle_l &= \sum_\beta \frac{\overline{D}_\beta}{\Delta S} \frac{d}{dt} \psi_k(\mathbf{X}_\beta), \\ &= \sum_\beta \frac{\overline{D}_\beta}{\Delta S} \dot{\mathbf{X}}_\beta \cdot \nabla \psi_k(\mathbf{X}_\beta), \\ &= - \sum_l M_{kl} \langle \nabla \cdot ([\tilde{\mathbf{u}}] \overline{D}) \rangle_l. \end{aligned}$$

□

This means that it is possible to take any reduced Lagrangian $l(\mathbf{u}, D)$ and, following the procedure described above, obtain a finite-dimensional canonical Hamiltonian system with approximate Lagrangian $\hat{L} \approx l$ for a set of particles, which may be interpreted on the grid as a discrete form of the EP equations resulting from l . If this system is integrated in time using a symplectic method, then the spatially-discretised Hamiltonian will be approximately preserved for long time-intervals. Suitable symplectic methods are discussed in the next section.

4 Symplectic time integration methods

In order to make a useful and practical Hamiltonian numerical method, it is necessary to choose the symplectic time-integrator carefully. In order to preserve the symplectic form, many integrators have to be implicit; often the expense of solving the resulting algebraic equations means that the symplectic integrator cannot compete with non-conservative schemes. In this section we suggest a practical first-order symplectic scheme for solving the semidiscretised system obtained using the method of the previous section. In order to do this, we restrict to a smaller set of problems where the Lagrangian takes the form

$$\mathcal{L} = \int \mathcal{K}(D, \mathbf{u}) - \mathcal{V}(D) d^n x,$$

where the nonlinear operator \mathcal{K} is interpreted as the kinetic energy and \mathcal{V} is the potential energy; we shall further require that \mathcal{K} takes the form

$$\mathcal{K} = \frac{1}{2} D \mathbf{u} \cdot \mathcal{B} \mathbf{u},$$

where \mathcal{B} is a linear operator, so that $\mathbf{m} = \mathcal{B}^{-1} \mathbf{u}$. This set represents a very large number of fluid systems so is not too much of a restriction (in the examples we shall also consider the EPDiff equation which does not have the density factor). We shall proceed by discretising \mathcal{L} :

$$\hat{L} = \sum_{kl} M_{kl} \left(\frac{1}{2} D_l \mathbf{u}_l \cdot \sum_m (\hat{B}^{-1})_{lm} \mathbf{u}_m - \hat{V}_l(\tilde{D}) \right).$$

For a given time step size Δt , write

$$\mathbf{X}_\beta^n \approx \mathbf{X}_\beta(n\Delta t),$$

and similarly for $\overline{\mathbf{m}}$ etc. To further compact the notation write

$$[\tilde{f}]_\beta^n = \sum_k \tilde{f}_k \psi(\mathbf{X}_\beta^n), \quad \langle \tilde{f} \rangle_k^n = \sum_\beta \tilde{f}_\beta \psi(\mathbf{X}_\beta^n),$$

and adopt similar notation for the gradient operators. We shall also write $\mathbf{U}_k([\overline{\mathbf{m}}], \tilde{D})$ as the solution to

$$\langle \overline{\mathbf{m}} \rangle_k = \nabla_{\mathbf{u}_k} \hat{L}(\mathbf{U}(\langle \overline{\mathbf{m}} \rangle, \tilde{D}), \tilde{D}),$$

i.e. the grid momentum-to-velocity map, so that

$$\hat{K}_l = \frac{1}{2} \langle \bar{\mathbf{m}} \rangle_l \cdot \mathbf{U}_l(\langle \bar{\mathbf{m}} \rangle, \tilde{D}).$$

The (first-order) symplectic-Euler scheme then takes the form

$$\begin{aligned} \frac{\bar{\mathbf{m}}_\beta^{n+1} - \bar{\mathbf{m}}_\beta^n}{\Delta t} &= -[(\nabla \mathbf{U}(\langle \bar{\mathbf{m}}^{n+1} \rangle^n, \langle \bar{D} \rangle^n))^T]_\beta^n \cdot \bar{\mathbf{m}}_\beta^{n+1} \\ &\quad - \bar{D}_\beta \left[\nabla \frac{1}{2} \frac{\langle \bar{\mathbf{m}}^{n+1} \rangle^n}{\langle \bar{D} \rangle^n} \cdot \mathbf{U}(\langle \bar{\mathbf{m}}^{n+1} \rangle^n, \langle \bar{D} \rangle^n) \right]^n \\ &\quad - \bar{D}_\beta \left[\nabla \frac{\partial V}{\partial \bar{D}}(\langle \bar{D} \rangle^n) \right]^n, \\ \frac{\mathbf{X}_\beta^{n+1} - \mathbf{X}_\beta^n}{\Delta t} &= -[\mathbf{U}(\langle \bar{\mathbf{m}}^{n+1} \rangle^n, \tilde{D}^n)]_\beta^n, \end{aligned}$$

which is implicit in $\bar{\mathbf{m}}$ but not \mathbf{X} . The algebraic system for $\bar{\mathbf{m}}$ can be efficiently solved using the following iterative scheme:

$$\begin{aligned} \bar{\mathbf{m}}_\beta^{n+1,j+1} &= \bar{\mathbf{m}}_\beta^n - \Delta t [(\nabla \mathbf{U}(\langle \bar{\mathbf{m}}^{n+1,j} \rangle^n, \langle \bar{D} \rangle^n))^T]_\beta^n \cdot \bar{\mathbf{m}}_\beta^{n+1,j+1} \\ &\quad - \Delta t \bar{D}_\beta \left[\nabla \frac{1}{2} \frac{\langle \bar{\mathbf{m}}^{n+1,j+1} \rangle^n}{\langle \bar{D} \rangle^n} \cdot \mathbf{U}(\langle \bar{\mathbf{m}}^{n+1,j} \rangle^n, \langle \bar{D} \rangle^n) \right]^n \\ &\quad - \Delta t \bar{D}_\beta \left[\nabla \frac{\partial \hat{V}}{\partial \bar{D}}(\langle \bar{D} \rangle^n) \right]^n, \end{aligned}$$

where $\bar{\mathbf{m}}_\beta^{n,j}$ is the j th element of the sequence converging to $\bar{\mathbf{m}}_\beta^n$ (with the sequence initialised with $\bar{\mathbf{m}}_\beta^{n,0} = \bar{\mathbf{m}}_\beta^{n-1}$). This results in inverting a sparse matrix (with number of non-zero elements proportional to the number of particles) each iteration (and for the case $\hat{V} = 0$ the matrix becomes block diagonal as the different particles decouple).

A second-order symplectic discretisation can be obtained by using the second-order Lobatto IIIa-b partitioned Runge-Kutta method as discussed in (Rei99) with reference to adaptive symplectic methods for molecular dynamics.

5 Examples

5.1 Example: the shallow-water- α equations

In this section we derive a Hamiltonian particle-mesh semidiscretisation for the shallow-water- α (SW- α) equations. These equations are obtained by decomposing Lagrangian particle trajectories into mean and fluctuating parts, averaging along those trajectories, and then applying the “frozen turbulence” Taylor assumption, before finally assuming isotropic, homogeneous turbulence statistics (Hol99).

The model is derived from the reduced Lagrangian

$$l = \int \frac{D}{2} (|\mathbf{u}|^2 + \alpha^2 |\nabla \mathbf{u}|^2 - gD) d^2x,$$

where α is the mean lengthscale for the fluctuations. The variational derivatives are

$$\frac{\delta l}{\delta \mathbf{u}} = (D + \nabla \cdot D \nabla) \mathbf{u}, \quad \frac{\delta l}{\delta D} = \frac{1}{2} (|\mathbf{u}|^2 + \alpha^2 |\nabla \mathbf{u}|^2) - gD,$$

and substituting these derivatives into the EP equation

$$\partial_t \mathbf{m} + (\nabla \mathbf{u})^T \cdot \frac{\delta l}{\delta \mathbf{u}} + \nabla \cdot \left(\mathbf{u} \frac{\delta l}{\delta \mathbf{u}} \right) = D \nabla \frac{\delta l}{\delta D},$$

gives the equations

$$\partial_t \mathbf{m} + \mathbf{u} \cdot \nabla \mathbf{m} + (\nabla \mathbf{u})^T \cdot \mathbf{m} + \mathbf{m} \nabla \cdot \mathbf{u} = D \nabla \left(-gD + \right.$$

$$\begin{aligned}
& \frac{1}{2} (|\mathbf{u}|^2 + \alpha^2 |\nabla \mathbf{u}|^2) \Big), \\
D_t + \nabla \cdot (D\mathbf{u}) &= 0, \\
\mathbf{m} &= (D - \alpha^2 \nabla \cdot D \nabla) \mathbf{u}.
\end{aligned} \tag{8}$$

In these equations the momentum \mathbf{m} is advected by the velocity \mathbf{u} obtained by inverting equation (8). The equations have a more familiar appearance in the form

$$\begin{aligned}
(\partial_t + \mathbf{u} \cdot \nabla)(1 - \alpha^2 D^{-1} \nabla \cdot D)^{-1} \mathbf{u} + (\nabla \mathbf{u})^T \cdot (1 - \alpha^2 D^{-1} \nabla \cdot D)^{-1} \mathbf{u} \\
= \nabla \left(-gD + \frac{1}{2} (|\mathbf{u}|^2 + \alpha^2 |\nabla \mathbf{u}|^2) \right), \\
D_t + \nabla \cdot (\mathbf{u}D) = 0,
\end{aligned}$$

which become the shallow-water equations

$$(\partial_t + \mathbf{u} \cdot \nabla) \mathbf{u} = -g \nabla D, \quad D_t + \nabla \cdot (\mathbf{u}D) = 0,$$

when α^2 is set to zero, making use of the identity

$$\nabla \frac{1}{2} |\mathbf{u}|^2 = (\nabla \mathbf{u}) \cdot \mathbf{u}.$$

Following the procedure set out in section 3, we discretise the Lagrangian using a piecewise-linear Galerkin finite element discretisation (see (Red93) for example). The Galerkin expansion for a function f given on grid points is

$$f(\mathbf{x}) = \sum_k N_k(\mathbf{x}) f_k,$$

where N_k is a continuous basis function which satisfies

$$N_i(\mathbf{x}_j) = \delta_{ij}.$$

Under this scheme, the Lagrangian becomes

$$\hat{L} = \sum_{kl} \left(\frac{1}{2} \tilde{\mathbf{u}}_k \cdot B_{kl} \tilde{\mathbf{u}}_k - \frac{1}{2} g \tilde{D}_k M_{kl} \tilde{D}_l \right),$$

where the Helmholtz matrix B takes the form

$$B_{ij} = \int_{\Omega} \sum_k \tilde{D}_k N_k(\mathbf{x}) (N_i(\mathbf{x}) N_j(\mathbf{x}) + \alpha^2 \nabla N_i(\mathbf{x}) \cdot \nabla N_j(\mathbf{x})) d^2 x,$$

and the mass matrix M takes the form

$$M = \int_{\Omega} N_i(\mathbf{x}) N_j(\mathbf{x}) d^2 x. \tag{9}$$

Both \hat{B} and M are sparse, well-conditioned, symmetric matrices so they are very quick to invert using a preconditioned conjugate gradients algorithm.

Using the Legendre transform, the momentum \tilde{m}_k on the grid is

$$\tilde{m}_k = \frac{\partial \hat{L}}{\partial \tilde{\mathbf{u}}_k} = \sum_l B_{kl} \tilde{\mathbf{u}}_l,$$

and the discrete Hamiltonian takes the form

$$\hat{H} = \sum_{kl} \left(\frac{1}{2} \tilde{m}_k \cdot (M_{kl} \sum_m B^{-1})_{lm} \tilde{m}_m + \frac{1}{2} g \tilde{D}_k M_{kl} \tilde{D}_l \right).$$

The canonical equations derived from the Hamiltonian \hat{H} are then

$$\dot{\mathbf{X}}_{\beta} = [\tilde{\mathbf{u}}]_{\beta} = [B^{-1} \langle \tilde{\mathbf{m}} \rangle]_{\beta},$$

$$\frac{\dot{\bar{\mathbf{m}}}_\beta}{D_\beta} = -[(\nabla \tilde{\mathbf{u}})^T]_\beta \cdot \frac{\bar{\mathbf{m}}_\beta}{D_\beta} - g[\nabla \tilde{D}]_\beta - \left[\nabla \frac{1}{2} \frac{\langle \bar{\mathbf{m}} \rangle}{\langle \bar{D} \rangle} \cdot B^{-1} \langle \bar{\mathbf{m}} \rangle \right]_\beta,$$

and the momentum equation on the grid take the form

$$\frac{d}{dt} \langle \bar{\mathbf{m}} \rangle_k + \langle \nabla \cdot ([\tilde{\mathbf{u}}] \bar{\mathbf{m}}) \rangle_k + \langle [(\nabla \tilde{\mathbf{u}})^T] \cdot \bar{\mathbf{m}} \rangle_k = - \left\langle \bar{D} \left[\nabla \left(gD + \frac{1}{2} \frac{\langle \bar{\mathbf{m}} \rangle}{\langle \bar{D} \rangle} \cdot \tilde{\mathbf{u}} \right) \right] \right\rangle_k,$$

We can also make a semidiscretisation for the Euler- α equations by removing the potential energy term and setting a constraint

$$D(\mathbf{x}_k) = 1, \quad k = 1, \dots, m,$$

via a set of Lagrange multipliers which give the pressure at each grid-point. It is possible to construct symplectic integrators for constrained Hamiltonian systems of this type (Jay96; LS94; Rei96) and these methods have already been applied to enforcing an incompressibility constraint in (CFR03).

5.2 Example: the 2D EP-Diff equations

The EP-Diff equations (HM05) are the generalisation to n -dimensional space of the Camassa-Holm equation (CH93), and represent the geodesic equations of motion for the H^1 norm. They represent the prototype for the family of regularised equations such as Euler- α (Hol99; MRS00), although they also have applications in computational anatomy and image processing (MTY02; Mum98).

The 2D EP-Diff equation is obtained from the reduced Lagrangian:

$$l = \int \frac{|\mathbf{u}|^2}{2} + \alpha^2 \frac{|\nabla \mathbf{u}|^2}{2} d^2x,$$

where α is a constant lengthscale parameter, and so the equation of motion is

$$\partial_t \mathbf{m} + \mathbf{u} \cdot \nabla \mathbf{m} + (\nabla \mathbf{u})^T \cdot \mathbf{m} + \mathbf{m} \nabla \cdot \mathbf{u} = 0, \quad \mathbf{m} = (1 - \alpha^2 \Delta) \mathbf{u}.$$

Following the programme set out in section 3 with a Galerkin finite element approximation, the discrete Lagrangian takes the form

$$\hat{L} = \sum_{kl} \frac{1}{2} \tilde{\mathbf{u}}_k \cdot (A_{kl} \tilde{\mathbf{u}}_l).$$

where the matrix A is the discrete inverse modified Helmholtz operator

$$A_{kl} = \int_{\Omega} N_k(\mathbf{x}) N_l(\mathbf{x}) + \alpha^2 \nabla N_k(\mathbf{x}) \cdot \nabla N_l(\mathbf{x}) d^2x.$$

The discrete Hamiltonian in Eulerian coordinates on the grid is then:

$$H = \sum_{kl} \frac{1}{2} \tilde{\mathbf{m}}_k \cdot \sum_m (A^{-1})_{km} M_{ml} \tilde{\mathbf{m}}_l,$$

where M_{kl} is the finite element mass matrix given by equation (9).

The canonical equations for this Hamiltonian are then

$$\begin{aligned} \dot{\mathbf{X}}_\beta &= [\mathbf{U}(\langle \bar{\mathbf{m}} \rangle)]_\beta = [A^{-1} \langle \bar{\mathbf{m}} \rangle]_\beta, \\ \frac{\dot{\bar{\mathbf{m}}}_\beta}{D_\beta} &= -[(\nabla \mathbf{U}(\langle \bar{\mathbf{m}} \rangle))^T]_\beta \cdot \mathbf{m}_\beta, \end{aligned}$$

and the equation for \mathbf{m} is the EP-Diff equations represented in our discrete calculus.

The symplectic Euler method with these equations is

$$\begin{aligned} \frac{\bar{\mathbf{m}}_\beta^{n+1} - \bar{\mathbf{m}}_\beta^n}{\Delta t} &= -[(\nabla \mathbf{U}(\langle \bar{\mathbf{m}}^{n+1} \rangle^n))^T]_\beta^n \cdot \bar{\mathbf{m}}_\beta^{n+1} \\ \frac{\mathbf{X}_\beta^{n+1} - \mathbf{X}_\beta^n}{\Delta t} &= [\mathbf{U}(\langle \bar{\mathbf{m}}^{n+1} \rangle^n)]_\beta^n, \end{aligned}$$

and the iterative scheme to solve for $\bar{\mathbf{m}}_\beta^{n+1}$ is

$$\bar{\mathbf{m}}_\beta^{n+1,j+1} = \bar{\mathbf{m}}_\beta^n - \Delta t [(\nabla \mathbf{U}(\langle \bar{\mathbf{m}}^{n+1,j} \rangle^n))^T]_\beta^n \cdot \bar{\mathbf{m}}_\beta^{n+1,j+1}. \quad (10)$$

Using this scheme only requires the inversion of one 3×3 matrix for each particle per iteration which leads to a very efficient method.

6 Numerical results

To demonstrate the particle-mesh approach, we give results using the method for the 2D EP-Diff equation described section 5.2 (numerical results and discussion of emergent behaviour for this system are given in (HS03)). The equations are solved in a $2\pi \times 2\pi$ periodic square, with $\alpha = 0.3133$. The discrete Lagrangian was obtained using piecewise-linear quadrilateral finite elements on a regular 128×128 grid and the particles positions were initialised 16 particles in each grid cell. The equations were integrated using Matlab using the HPM C-mex files (see <http://www.cwi.nl/projects/gi/HPM/>) to perform the grid-particle operations. The finite element matrices B and M were stored as sparse matrices and inverted using conjugate gradients with incomplete Cholesky preconditioning, reaching a residual of less than 1×10^{-9} in less than 10 iterations. The iterative scheme (10) converged with a total error of less than 1×10^{-9} in less than 3 iterations for each timestep (with $dt = 0.0204$) during the experiment.

The initial data had the momentum zero everywhere except for a thin strip near to $x = \pi$ with a sin-profile in the x -direction along that strip. The plots of x -velocity in figures 1-6 show the strip bending into a chevron/arrow shape before emitting a singular pulse corresponding to a Dirac δ -function in the momentum field. The numerical method still behaves well after the emergence of this singular spike as the Helmholtz operator (which is inverted to obtain the velocity on the grid) is discretised using piecewise linear finite elements and hence the method supports weak solutions. Eventually a second, smaller, spike is produced by the chevron; the equation is solved using periodic boundary conditions and so the larger peak catches up with the smaller one and they exchange momentum in a collision. This allows the second peak to move away.

A plot of the discrete Hamiltonian during the numerical experiment is shown in figure 7. This plot illustrates that, as the timestepping method used is symplectic, the discrete Hamiltonian is conserved within $\mathcal{O}(\Delta t)$ of the initial value at time $t = 0$ for very long time-intervals. This is the real benefit of discretising the variational structure of the equations.

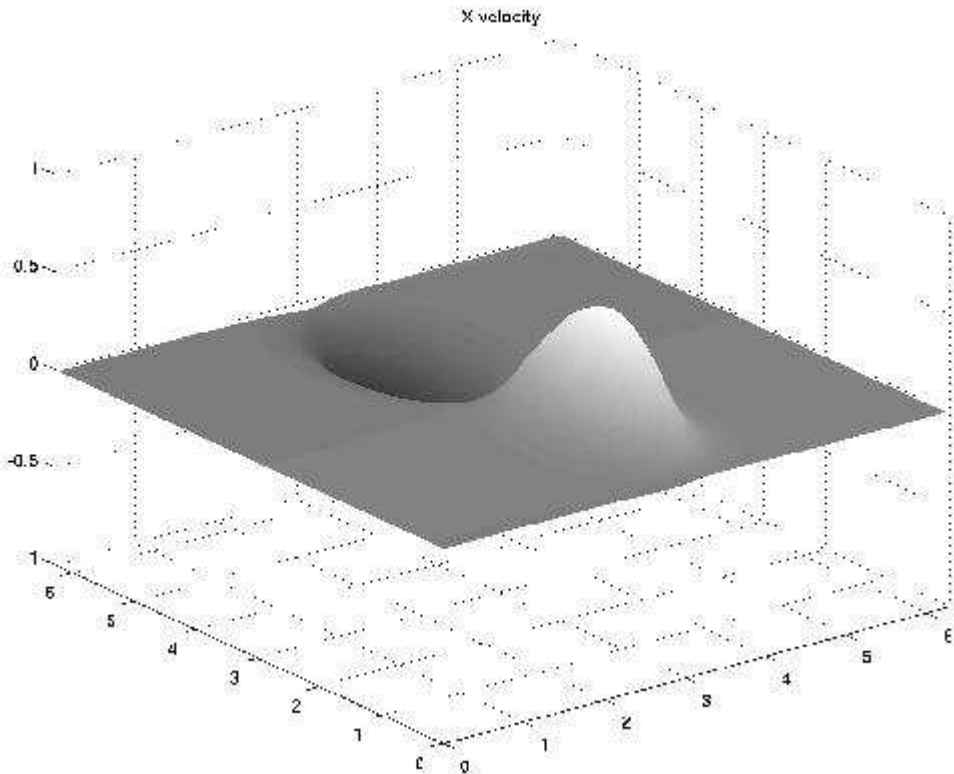


Figure 1: Plot of x -velocity at $t = 0$. The momentum is confined to a strip along $x = \pi$ with a sin-profile, and the velocity has the resulting distribution after the application of the inverse Helmholtz operator.

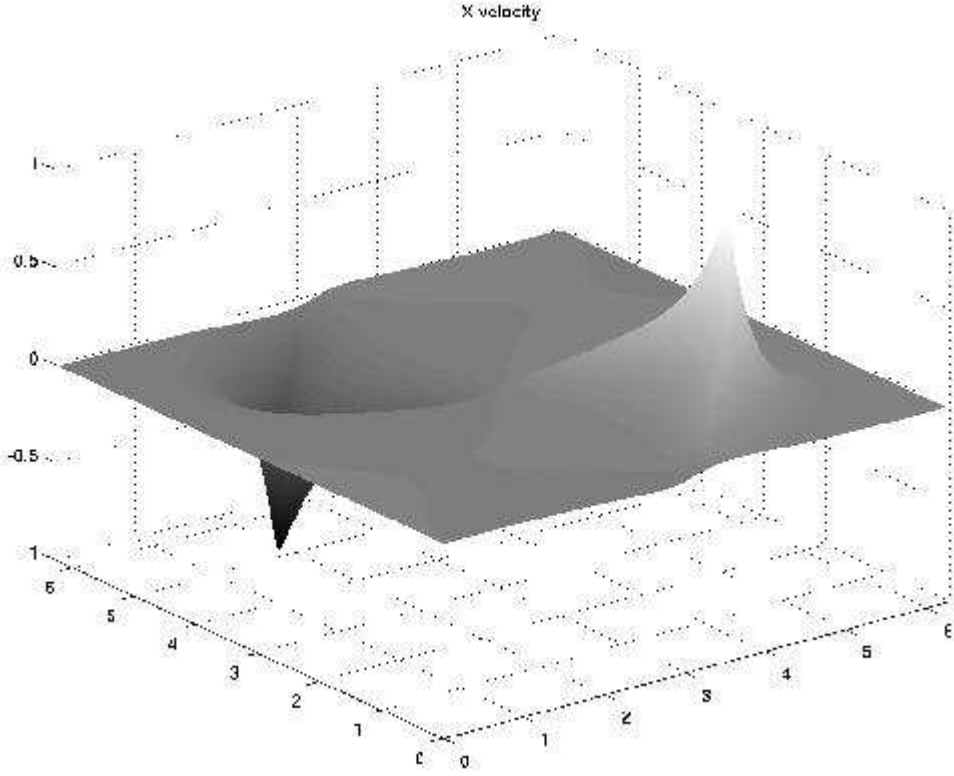


Figure 2: Plot of x -velocity at $t = 4.48$. The shear profile has pulled the wave out into a chevron shape with an accumulation of velocity at the head. A peak with discontinuous gradient has formed but this does not cause problems numerically as the finite element discretisation on the grid supports weak solutions.

7 Discussion and outlook

We introduced a general framework for deriving canonical Hamiltonian semi-discretised equations from the reduced Lagrangian in Eulerian coordinates, based on the particle-mesh approach. This framework has several advantages:

- The use of Lagrangian particles in the discretisation means that the equations are always canonical. This means that the discrete structure operator is guaranteed to satisfy the Jacobi identity and so a symplectic time integrator can be used, leading to long-time preservation of the Hamiltonian. The canonical structure also makes for easier discussion of adiabatic invariants in the discrete system (Cot04).
- The Hamiltonian is given in terms of Eulerian coordinates. This means it is easy to add on extra physics, make approximations, *etc.* Many models, such as those discussed in section 5, involve differential operators given in Eulerian coordinates which become rather complicated and “entangled” in the Lagrangian variables. This approach avoids this problem.
- This approach allows the momentum densities to become δ -functions in the limit, whilst the velocities on the grid can be represented using finite elements which means that weak solutions can be discussed, for example in the EP-Diff equations we seek solutions in H^1 (as illustrated in the numerical example).
- The symplectic Euler method can be efficiently applied to integrate the spatially-discrete equations in space. It should also be possible to obtain higher-order symplectic methods for greater accuracy.

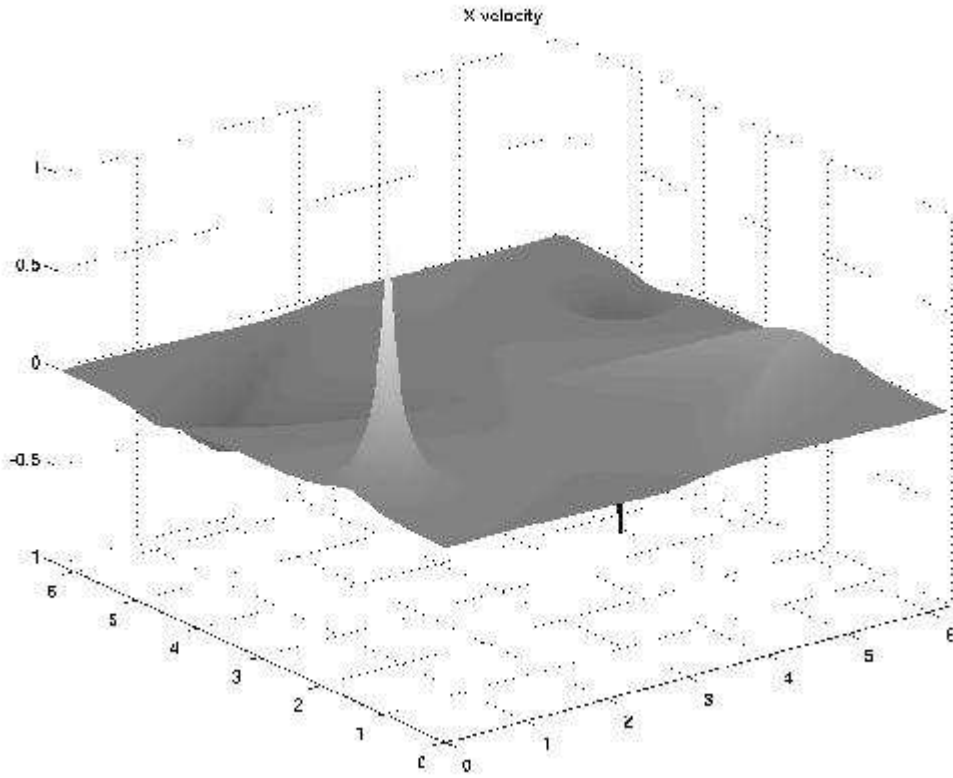


Figure 3: Plot of x -velocity at $t = 8.55$. The peak has separated from the chevron and is propagating at a higher speed. The problem is solved using periodic boundary conditions; the peak “wraps round” to the other side of the domain.

- The numerical experiment demonstrates that, at least for the EP-Diff equations, this numerical method is computationally feasible and produces well-behaved numerical solutions.

Future work may take several different directions, including:

- Development of higher-order symplectic integrators for these models in order to produce practical methods.
- Application to other fluid models: the two-layer Green-Naghdi equations (CC99), the quasi-geostrophic equations (HZ98), rotating shallow-water- α , Euler-Boussinesq- α in 3D (Hol99) *etc.*
- Comparison of methods with existing schemes for simple models such as the EP-Diff equations in 1, 2 and 3 dimensions.
- Investigation of the effects of smoothing in the shallow-water- α equations. Does the smoothing in the velocity field keep the solution well-behaved over long time intervals?
- Use of normal-form theory, following the work in (Cot04), to investigate geostrophic balance in the numerical scheme for the rotating shallow-water- α equations, and other rotating models.
- Comparison of the solutions of shallow-water- α obtained using the method given in this paper with solutions of RLDSW obtained using the HPM method.
- Inclusion of boundary conditions: the approach, as described here, only works on a closed manifold (such as the 2-torus *i.e.* a square with periodic boundary conditions).
- Obtain an extension to semi-direct product systems with other types of advected quantities (other than densities) such as scalars, vectors, and higher-order tensors.

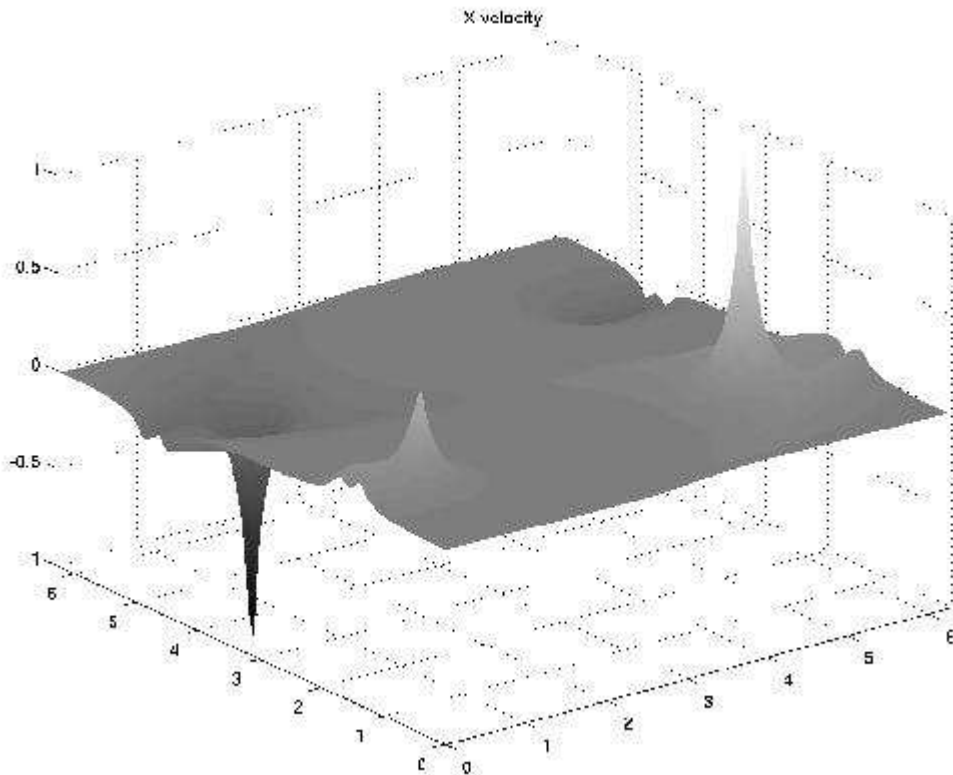


Figure 4: Plot of x -velocity at $t = 16.70$. A second peak is forming at the head of the chevron.

Acknowledgements: Thanks to Sebastian Reich, Darryl Holm and Joel Fine for their useful discussions during the writing of this paper, to Jason Frank for the use of his HPM C-mex code, to Matthew Piggott for advice on programming the finite element method, to the Daniels family of Ohio for their generous hospitality during the early stages of this work, and to NERC for funding under grant number NER/T/S/2002/00459.

References

- G. Benettin and A. Giorgilli. On the Hamiltonian interpolation of near-to-the-identity symplectic mappings with application to symplectic integration algorithms. *Journal of Statistical Physics*, 74(5/6):1117–1143, March 1994.
- T.J. Bridges and S. Reich. Multi-symplectic integrators: numerical schemes for Hamiltonian PDEs that conserve symplecticity. *Physics Letters A*, 284:184–193, 2001.
- W. Choi and R. Camassa. Fully nonlinear internal waves in a two-fluid system. *Journal of Fluid Mechanics*, 396:1–36, October 1999.
- C.J. Cotter, J. Frank, and S. Reich. Hamiltonian particle-mesh method for two-layer shallow-water equations subject to the rigid-lid approximation. *SIAM Journal on Applied Dynamical Systems*, 3(1):69–83, 2003.
- R. Camassa and D.D. Holm. An integrable shallow-water equation with peaked solitons. *Physical Review Letters*, 71(11):1661–1664, September 1993.
- A. Chorin. Numerical study of slightly viscous flow. *Journal of Fluid Mechanics*, 57:785–796, 1973.
- G. Cottet and P. Koumoutsakos. *Vortex Methods: Theory and Practice*. CUP, Cambridge, 2000.

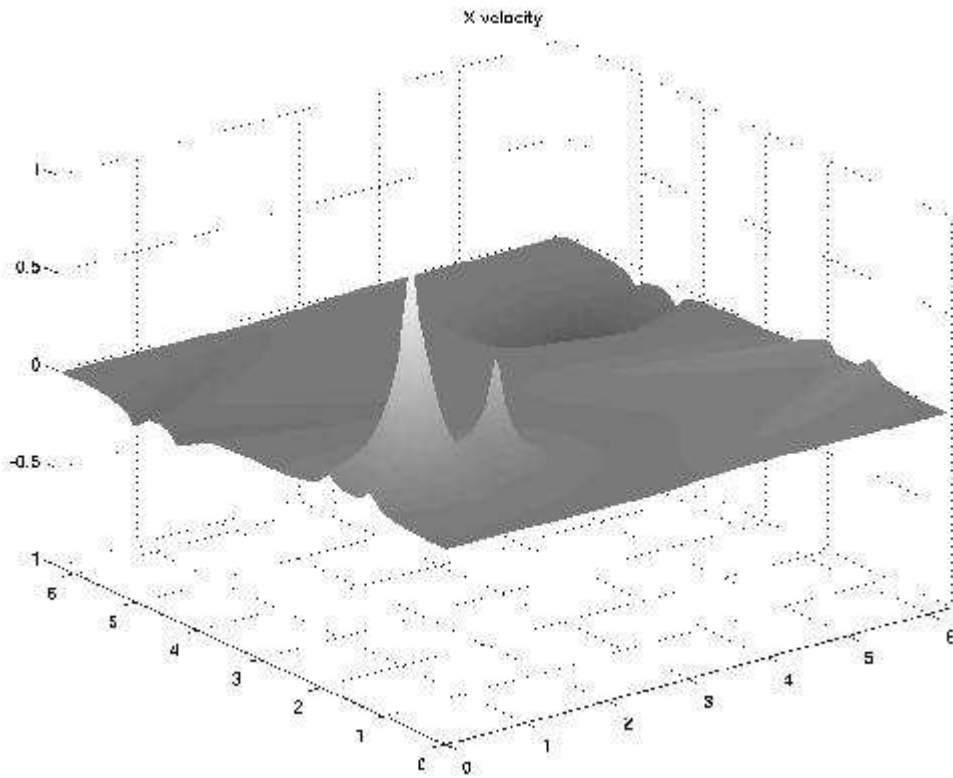


Figure 5: Plot of x -velocity at $t = 20.78$. The first peak is larger than the second peak; it starts to catch up.

- C.J. Cotter. *Model Reduction for Shallow-Water Dynamics: Balance, Adiabatic Invariance and Subgrid Modelling*. PhD thesis, Imperial College London, 2004.
- C.J. Cotter and S. Reich. Adiabatic invariance and applications to MD and NW. *BIT*, 44:439–455, 2004.
- C.J. Cotter and S. Reich. Geometric integration of a weak-wave model. *Applied Numerical Mathematics*, 48:293–305, 2004.
- C. de Boor. *A Practical Guide to Splines*. Springer-Verlag, 1978.
- J. Frank, G. Gottwald, and S. Reich. A Hamiltonian particle-mesh method for the rotating shallow-water equations. In *Lecture Notes in Computational Science and Engineering*, volume 26, pages 131–142. Springer, Heidelberg, 2002.
- J. Frank and S. Reich. The Hamiltonian particle mesh method for the spherical shallow-water equations. *Atmospheric Science Letters*, pages 89–95, 2004.
- R.A. Gingold and J.J. Monaghan. Smoothed particle hydrodynamics: theory and application to non-spherical stars. *Mon. Not. R. Astr. Soc.*, 181:375–389, 1977.
- E. Hairer. Backward error analysis of numerical integrators and symplectic methods. *Annals of Numerical Mathematics*, 1:107–132, 1994.
- E. Hairer and C. Lubich. The life-span of backward error analysis for numerical integrators. *Numer. Math.*, 76(4):441–462, 1997.
- E. Hairer, C. Lubich, and G. Wanner. *Geometric Numerical Integration: Structure-Preserving Algorithms for Ordinary Differential Equations*. Springer, Heidelberg, 2002.

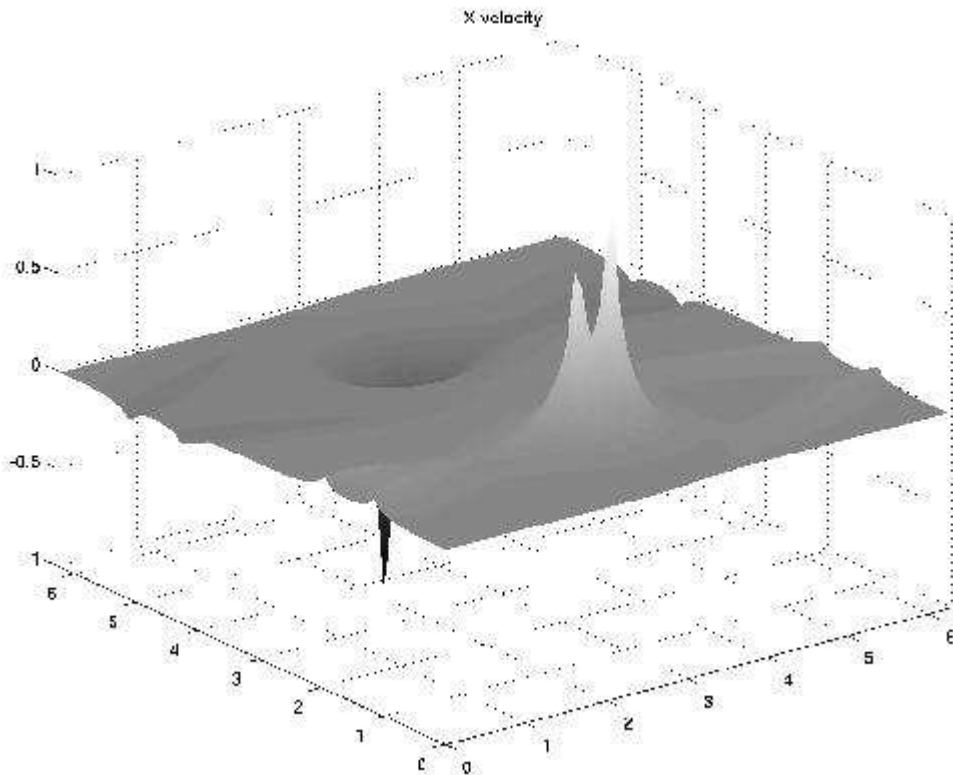


Figure 6: Plot of x -velocity at $t = 24.85$. The first peak is just behind the second peak and they have exchanged momentum in a “collision”, allowing the second peak to accelerate away.

- D.D. Holm and J. Marsden. Momentum maps and measure-valued solutions (peakons, filaments, and sheets) for the EPDiff equation. In J.E. Marsden and T.S. Ratiu, editors, *The Breadth of Symplectic and Poisson Geometry: Festschrift in Honor of Alan Weinstein*, Progress in Mathematics. Springer-Verlag, 2005.
- D.D. Holm, J.E. Marsden, and T.S. Ratiu. The Euler-Poincaré equations and semidirect products with applications to continuum theories. *Advances in Mathematics*, 137(1):1–81, July 1998.
- D.D. Holm, J.E. Marsden, and T.S. Ratiu. The Euler-Poincaré equations in geophysical fluid dynamics. In *Isaac Newton Institute Proceedings*, 1998.
- D.D. Holm. Fluctuation effects on 3D Lagrangian mean and Eulerian mean fluid motion. *Physica D*, 133:215–269, 1999.
- D.D. Holm. The Euler-Poincaré dynamics of perfect complex fluids. In *Geometry, Mechanics and Dynamics*, pages 113–167. Springer-Verlag, 2002. Special Volume in Honor of the 60th Birthday of J.E. Marsden.
- D. D. Holm and M. F. Staley. Wave structure and nonlinear balances in a family of evolutionary PDEs. *SIAM Journal on Applied Dynamics Systems*, 2(3):323–380, 2003.
- D.D. Holm and V. Zeitlin. Hamilton's principle for quasigeostrophic motion. *Phys. Fluids*, 10(4), 1998.
- L.O. Jay. Symplectic partitioned Runge-Kutta methods for constrained Hamiltonian systems. *SIAM J. Numer. Anal.*, 33:368–387, 1996.
- B. Leimkuhler and S. Reich. *Simulating Hamiltonian Dynamics*. CUP, 2005.
- B. Leimkuhler and R.D. Skeel. Symplectic numerical integrators in constrained Hamiltonian systems. *J. Comput. Phys.*, 112:117–125, 1994.

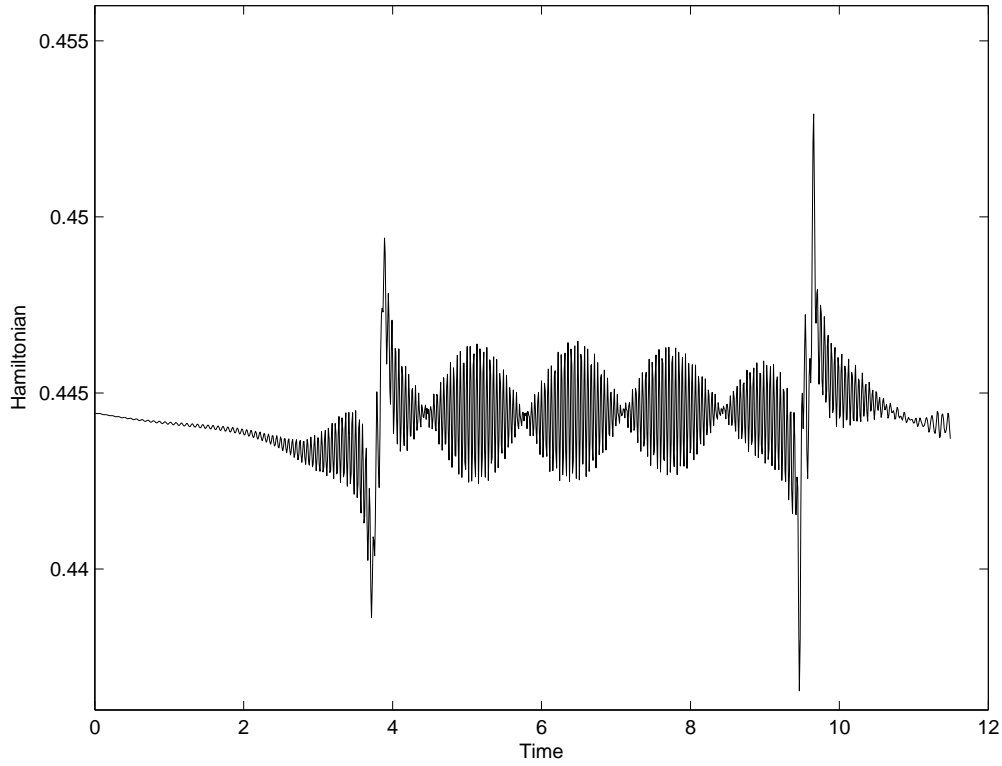


Figure 7: Plot of the Hamiltonian against time during the numerical experiment. The time stepping method is symplectic and so the Hamiltonian stays within $\mathcal{O}(\Delta t)$ of the value at $t = 0$ for very long time-intervals.

- L.B. Lucy. A numerical approach to the testing of the fission hypothesis. *The Astronomical Journal*, 82:1013–1024, 1977.
- R.I. McLachlan. On the numerical integration of ODEs by symmetric composition methods. *Physica D*, 133:215–269, 1999.
- J. Marsden, G. Patrick, and S. Shkoller. Multisymplectic geometry, variational integrators, and nonlinear PDEs. *Comm. Math. Phys.*, 199:351–391, 1998.
- J. Marsden, S. Pekarsky, S. Shkoller, and M. West. On a multisymplectic approach to continuum mechanics. *J. Geom. Phys.*, 38:253–284, 2001.
- B. Moore and S. Reich. Backward error analysis for multi-symplectic integration methods. *Numerische Mathematik*, 95:625–652, 2003.
- B. Moore and S. Reich. Multi-symplectic integration methods for Hamiltonian PDEs. *Future Generation Computer Systems*, 19:395–402, 2003.
- J.E. Marsden, T. Ratiu, and S. Shkoller. The geometry and analysis of the averaged Euler equations and a new diffeomorphism group. *Geom. Funct. Anal.*, 10:582–599, 2000.
- J.E. Marsden and S. Shkoller. Global well-posedness for the Lagrangian averaged Navier-Stokes (LANS- α) equations on bounded domains. *Phil. Trans. R. Soc. Lond. A*, 359:1449–1468, 2001.
- M.I. Miller, A. Trouné, and L. Younes. On the metrics and Euler-Lagrange equations of computational anatomy. *Annu. Rev. Biomed. Eng.*, 4:375–405, 2002.

- D. Mumford. *Questions Matheématiques En Traitement Du Signal et de L'Image*, chapter 3, pages 7–13. Institut Henri Poincaré, Paris, 1998.
- M. Oliver. Variational asymptotics for rotating shallow water near geostrophy: a transformational approach. submitted, 2005.
- M. Oliver and S. Shkoller. The vortex blob method as a second-grade non-Newtonian fluid. *Communications in Partial Differential Equations*, 22:295–314, 2001.
- M. Oliver, M. West, and C. Wulff. Approximate momentum conservation for spatial semidiscretizations of nonlinear wave equations. *Numerische Mathematik*, 97:493–535, 2004.
- J.N. Reddy. *Introduction to the Finite Element Method*. McGraw-Hill, 1993.
- S. Reich. Symplectic integration of constrained hamiltonian systems by composition methods. *SIAM J. Numer. Anal.*, 33:475–491, 1996.
- S. Reich. Backward error analysis for numerical integrators. *SIAM J. Numer. Anal.*, 36:1549–1570, 1999.
- S. Reich. Finite volume methods for multi-symplectic PDEs. *BIT*, 40:559–582, 2000.
- R. Salmon. Practical use of Hamilton's principle. *J. Fluid. Mech*, 132(431-444), 1983.
- S. Shkoller. The Lagrangian averaged Euler (LAE- α) equations with free-slip or mixed boundary conditions. In P. Holmes, P. Newton, and A. Weinstein, editors, *Geometry, Mechanics, and Dynamics*, pages 169–180. Springer-Verlag, 2002. Special Volume in Honor of the 60th Birthday of J.E. Marsden.
- V. Zeitlin. Finite-mode analogs of 2D ideal hydrodynamics: Coadjoint orbits and local canonical structure. *Physica D*, pages 353–362, 1991.

This figure "Frame001.jpg" is available in "jpg" format from:

<http://arxiv.org/ps/math/0501468v1>

This figure "Frame011.jpg" is available in "jpg" format from:

<http://arxiv.org/ps/math/0501468v1>

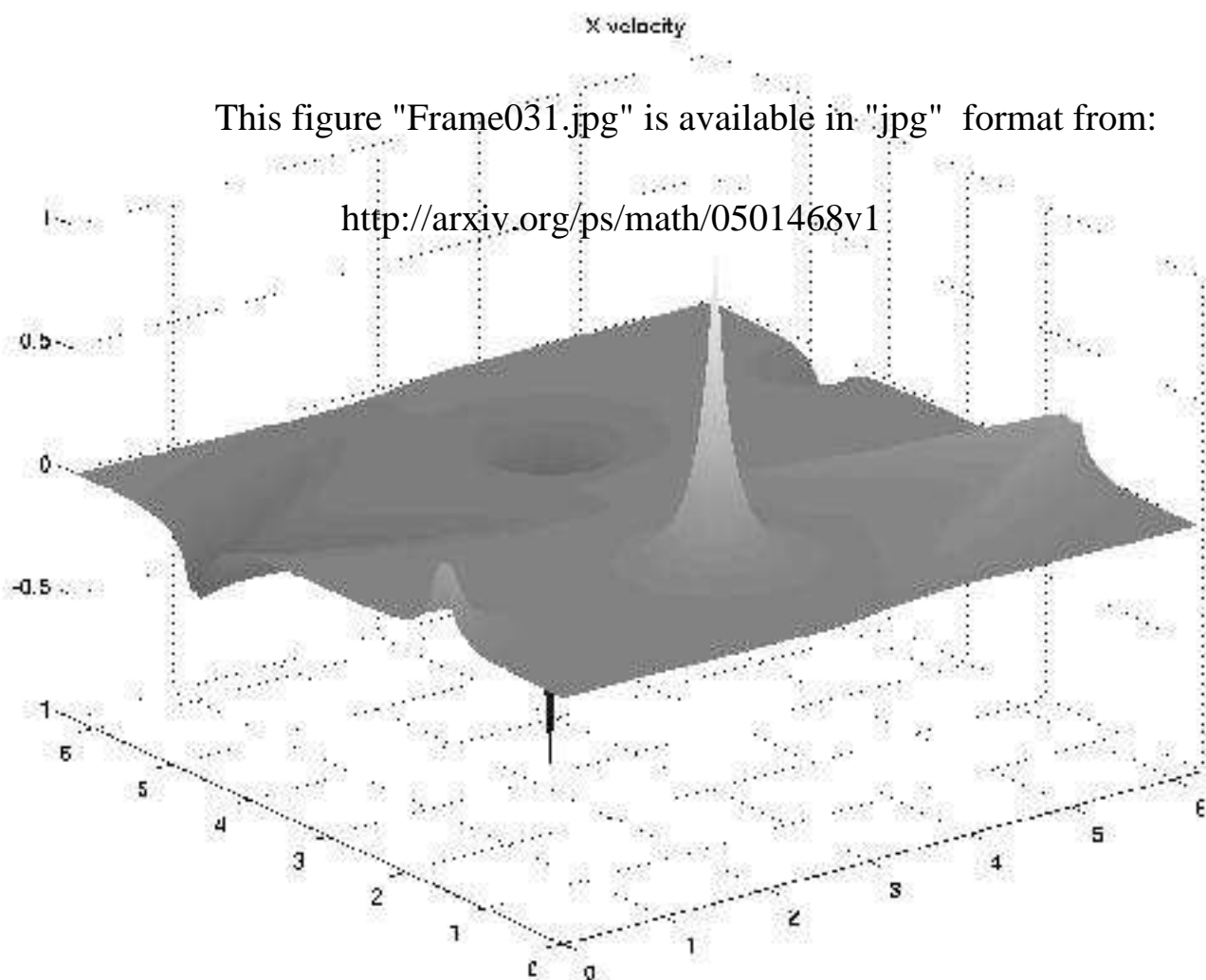
This figure "Frame021.jpg" is available in "jpg" format from:

<http://arxiv.org/ps/math/0501468v1>

X velocity

This figure "Frame031.jpg" is available in "jpg" format from:

<http://arxiv.org/ps/math/0501468v1>



This figure "Frame041.jpg" is available in "jpg" format from:

<http://arxiv.org/ps/math/0501468v1>

This figure "Frame051.jpg" is available in "jpg" format from:

<http://arxiv.org/ps/math/0501468v1>

This figure "Frame061.jpg" is available in "jpg" format from:

<http://arxiv.org/ps/math/0501468v1>